

1 Role of Coupled Dynamics in the Catalytic Activity of Prokaryotic-like 2 Prolyl-tRNA Synthetases

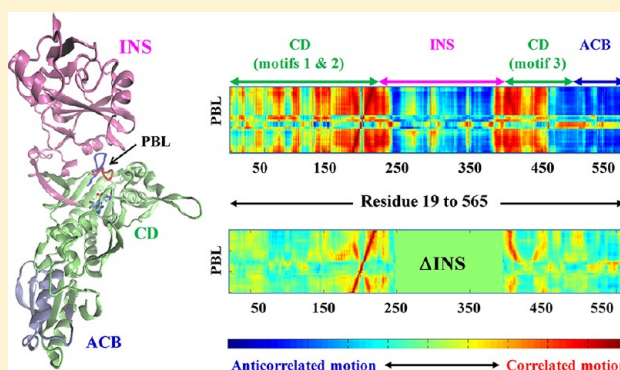
3 Brianne Sanford,^{†,‡} Bach Cao,[†] James M. Johnson,[†] Kurt Zimmerman,[†] Alexander M. Strom,[†]
4 Robyn M. Mueller,[†] Sudeep Bhattacharyya,^{*,†} Karin Musier-Forsyth,^{*,‡} and Sanchita Hati^{*,†}

5 [†]Department of Chemistry, University of Wisconsin–Eau Claire, Eau Claire, Wisconsin 54702, United States

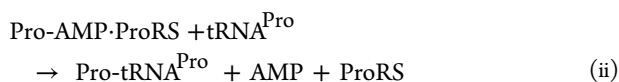
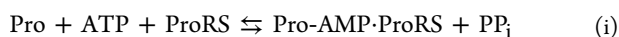
6 [‡]Department of Chemistry and Biochemistry, Center for RNA Biology, The Ohio State University, Columbus, Ohio 43210, United
7 States

8 **S** Supporting Information

9 **ABSTRACT:** Prolyl-tRNA synthetases (ProRSs) have been
10 shown to activate both cognate and some noncognate amino
11 acids and attach them to specific tRNA^{Pro} substrates. For
12 example, alanine, which is smaller than cognate proline, is
13 misactivated by *Escherichia coli* ProRS. Mischarged Ala-tRNA^{Pro}
14 is hydrolyzed by an editing domain (INS) that is distinct from
15 the activation domain. It was previously shown that deletion
16 of the INS greatly reduced cognate proline activation efficiency. In
17 this study, experimental and computational approaches were
18 used to test the hypothesis that deletion of the INS alters the
19 internal protein dynamics leading to reduced catalytic function.
20 Kinetic studies with two ProRS variants, G217A and E218A,
21 revealed decreased amino acid activation efficiency. Molecular
22 dynamics studies showed motional coupling between the INS and protein segments containing the catalytically important
23 proline-binding loop (PBL, residues 199–206). In particular, the complete deletion of INS, as well as mutation of G217 or E218
24 to alanine, exhibited significant effects on the motion of the PBL. The presence of coupled dynamics between neighboring
25 protein segments was also observed through in silico mutations and essential dynamics analysis. Altogether, this study
26 demonstrates that structural elements at the editing domain–activation domain interface participate in coupled motions that
27 facilitate amino acid binding and catalysis by bacterial ProRSs, which may explain why truncated or defunct editing domains have
28 been maintained in some systems, despite the lack of catalytic activity.



29 **P**rolyl-tRNA synthetases (ProRSs) are class II synthetases
30 that catalyze covalent attachment of proline to the 3'-end
31 of the tRNA^{Pro} in a two-step reaction:



32 ProRSs from all three kingdoms of life are known to misactivate
33 noncognate alanine and cysteine, resulting in mischarged
34 tRNA^{Pro}.^{1–3} To maintain high fidelity in protein synthesis,
35 some ProRSs have acquired editing mechanisms to prevent
36 misaminoacylation of tRNA^{Pro}.^{1,2,4} On the basis of sequence
37 alignments, ProRSs are classified into two broad groups:
38 “eukaryotic-like” and “prokaryotic-like”.^{5,6} *Escherichia coli* (Ec)
39 ProRS, a representative member of the prokaryotic-like group,
40 is a multidomain protein. The catalytic domain (motifs 1–3,
41 consisting of residues 64–81, 128–164, and 435–465,
42 respectively) catalyzes the activation of proline and the
43 aminoacylation of tRNA^{Pro}. The anticodon binding domain
44 (residues 506–570) is critical for reorganization of cognate
45 tRNA. The insertion domain (INS; residues 224–407, located

between motifs 2 and 3 of the catalytic domain) is the post-
46 transfer editing active site that hydrolyzes mischarged Ala-
47 tRNA^{Pro}.^{7,8} In contrast, Cys-tRNA^{Pro} is hydrolyzed by a free-
48 standing editing domain known as YbaK present in some
49 species.^{9,10} Unlike prokaryotic-like ProRSs, eukaryotic-like
50 ProRSs do not possess the INS but in some cases encode
51 free-standing editing domain homologues.
52

In addition to post-transfer editing, the INS of Ec ProRS was
53 found to have a significant impact on amino acid binding and
54 activation.¹¹ Deletion of the INS (residues 232–394) of Ec
55 ProRS resulted in a 200-fold increase in the K_M for proline. The
56 overall proline activation efficiency was reduced by ~1200-fold
57 relative to that of the wild-type (WT) enzyme.¹¹ Although the
58 specific reason for this drastic effect is not understood, circular
59 dichroism measurements demonstrated that deletion of the INS
60 has no significant effect on the overall folding of the mutant
61 protein.¹¹ Thus, it remains unclear what role the editing
62 domain plays in substrate binding and amino acid activation.
63

Received: July 22, 2011

64 It is known that for multidomain proteins like ProRS,
65 coupled domain dynamics play an important role in catalytic
66 function.^{12,13} Although the relevance of the editing domain to
67 amino acid activation by ProRS is not understood, a substrate-
68 induced conformational change of a neighboring loop, known
69 as the proline-binding loop (PBL, residues 199–206), was
70 revealed by structural studies.¹⁴ Three-dimensional structures
71 of two bacterial ProRSs, *Rhodospseudomonas palustris* ProRS (Rp
72 ProRS) and *Enterococcus faecalis* ProRS [Ef ProRS (Figure 1a)],
73 showed an induced-fit binding mode with a large displacement
74 (~7 Å) of the PBL upon binding of the prolyl-adenylate
75 analogue, 5'-O-[N-(prolyl)sulfamoyl] adenosine (Pro-AMS)

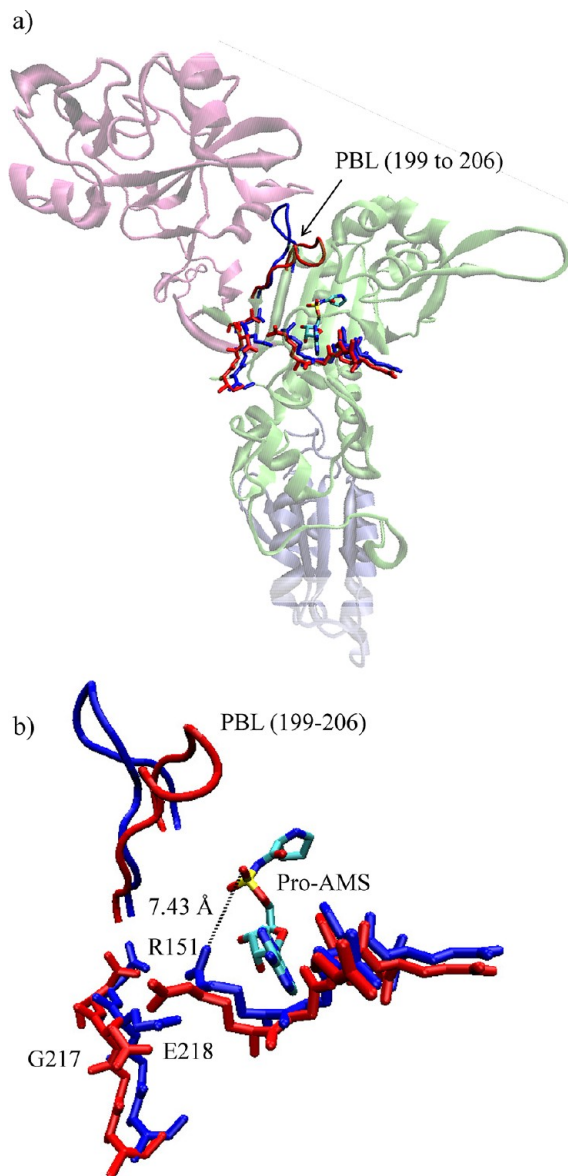


Figure 1. (a) Cartoon representation of the three-dimensional structure of the monomeric form of Ef ProRS (residues 1–570, PDB entry 2J3L, chain B). The structural domains are colored as follows: lime for the catalytic domain (residues 1–223 and 408–505), mauve for the editing domain (residues 224–407), and ice blue for the anticodon-binding domain (residues 506–570). The PBL is shown as tubes. G217, E218, R151, and the prolyl-adenylate analogue are shown as licorice: red for the “closed” state and blue for the “open” state. (b) Closer view of the PBL and the active site residues.

(Figure 1b).¹⁴ Comparison of the substrate-bound and
unbound structures also showed that the large displacement
of the PBL was associated with the reorientation of several
active site moieties, as well as some polypeptide segments that
belong to the catalytic domain–editing domain interface.¹⁴
These observations together with the observed dramatic change
in Ec ProRS function upon deletion of the editing domain led
us to hypothesize that the dynamics of structural elements
proximal to the PBL influence substrate binding and catalysis
by prokaryotic-like ProRSs.

To test the hypothesis described above, in this study the
coupling of motions among various structural elements of Ec
ProRS was investigated using computational and experimental
approaches. In particular, to examine the effect of INS on the
PBL dynamics, the motion of the full-length enzyme and the
truncated enzyme (constructed by deletion of INS, hereafter
termed ΔINS) was computationally simulated. Also, two highly
conserved residues of the prokaryotic-like ProRS family, G217
and E218 (Figure 2), were mutated. These two residues,

EcoliProRS	A	A	S	K	I	F	S	R	M	G	L	D	F	R	A	V	Q	A	I	G	S	I	G	G	S	A	S	H	E	F	Q	V	L	A	Q	S	E	E	D	D	V	F	S	D	T	S	D	Y	A	A	N	I	E	L	A	E	A	238		
SenteProRS	A	A	S	R	I	F	S	R	M	G	L	D	F	R	A	V	Q	A	I	G	S	I	G	G	N	A	S	H	E	F	Q	V	L	A	Q	S	E	E	D	D	V	F	S	D	V	S	D	Y	A	A	N	I	E	L	A	E	A	238		
HinfIProRS	Q	V	S	N	I	F	N	R	L	G	L	D	F	R	A	V	Q	A	I	G	S	I	G	G	S	A	S	H	E	F	Q	V	L	A	Q	S	E	E	D	D	V	F	S	T	S	D	F	A	A	N	I	E	L	A	E	A	238			
EfaecProRS	K	A	V	T	E	V	F	K	R	C	G	L	E	F	R	S	I	I	G	I	G	G	M	G	G	K	S	K	E	F	M	A	I	S	E	I	E	E	T	I	C	Y	S	T	S	D	Y	A	A	N	L	E	M	A	T	S	238			
EfcalProRS	K	A	V	S	R	I	F	E	R	C	G	L	E	F	R	A	I	I	G	I	G	G	M	G	G	K	S	K	E	F	M	A	I	S	E	I	E	E	T	I	C	Y	S	T	S	D	Y	A	A	N	L	E	M	A	T	S	238			
LreutProRS	K	A	Y	N	I	F	D	R	I	G	L	N	Y	K	V	L	A	I	S	G	T	M	G	G	K	S	Q	E	F	S	A	P	A	V	E	I	E	T	I	A	Y	-	T	D	G	D	Y	A	A	N	L	E	K	A	E	S	237			
BanthProRS	K	A	Y	S	N	I	F	A	R	C	G	L	N	F	R	A	V	I	A	I	S	G	T	M	G	G	K	T	H	E	F	M	V	L	S	D	V	E	I	T	I	A	Y	S	D	T	S	D	Y	A	A	N	L	E	M	A	F	V	238	
IpolyProRS	A	A	Y	T	R	I	F	E	R	C	G	L	N	F	R	S	V	E	A	I	S	G	I	G	G	S	S	Q	E	F	H	V	L	A	E	S	E	E	I	I	Y	D	C	S	C	G	Y	A	A	N	L	E	K	A	E	S	238			
CperfProRS	K	A	Y	V	N	I	F	N	R	C	G	L	D	A	K	A	V	A	A	I	S	G	I	G	G	S	S	A	E	F	M	V	K	S	E	V	E	E	D	D	V	F	T	A	C	D	Y	A	A	N	L	E	K	A	P	S	238			
MtubrProRS	E	A	Y	O	R	I	F	D	R	L	O	V	R	V	V	I	S	V	A	V	S	G	A	M	G	G	S	R	S	E	E	F	L	A	E	S	P	S	E	E	I	A	F	V	R	C	L	E	S	G	Y	A	A	N	V	E	A	V	T	240

Figure 2. Portion of the multiple-sequence alignment of 10 prokaryotic-like ProRSs. The PBL and the highly conserved ²¹⁷GED²¹⁹ motif are boxed.

located at the junction of the activation domain and the editing
domain, are not directly involved in catalysis but undergo
substrate-induced conformational changes.¹⁴ To evaluate the
effect of mutation of these noncatalytic conserved residues on
PBL dynamics and enzyme catalysis, enzyme motions were
computationally simulated and kinetic parameters were
determined experimentally. Taken together, the results of this
study shed light on the role of distant domains and noncatalytic
residues in producing a catalytically competent state for amino
acid binding and activation by prokaryotic-like ProRSs.

MATERIALS AND METHODS

All experimental studies were performed using purified Ec
ProRS. Because Ec and Ef ProRS possess a high degree of
sequence identity (48%), computational studies were per-
formed starting with the X-ray crystallographic structure of Ef
ProRS [PDB entry 2J3M (“open” state)],¹⁴ and the results
were compared with results using a homology model of Ec
ProRS developed using Ef ProRS as a template (provided by S.
Cusack). All simulations were performed with apoenzymes.

EXPERIMENTAL METHODS

Materials. All amino acids (Sigma) were of the highest
quality (>99% pure) and used without further purification.
Tritiated proline (83 Ci/mmol) and alanine (75 Ci/mmol)
were from Perkin-Elmer. Primers for site-directed mutagenesis
and polymerase chain reaction were from Integrated DNA
Technologies.

Enzyme Preparation. Overexpression and purification of
histidine-tagged WT and mutant Ec ProRS were performed as

described previously.^{15,16} Plasmids encoding G217A and E218A Ec ProRS were generated by QuikChange mutagenesis (Stratagene) of pCS-M1S¹⁶ using the following primers: G217A, 5'-GCG CAG AGC GCG GAA GAC GAT GTG G-3' (top) and 5'-CCA CAT CGT CTT CCG CGC TCT GCG C-3' (bottom); E218A, 5'-GCG CAG AGC GGT GCG GAC GAT GTG G-3' (top) and 5'-CAA CAT CGT CCG CAC CGC TCT GCG C-3' (bottom). Results of mutagenesis were confirmed by DNA sequencing (University of Wisconsin, Biotechnology Center, Madison, WI). Protein expression was induced in Ec SG13009 (pREP4) competent cells with 1 mM isopropyl β -D-thiogalactoside for 4 h at 37 °C. Histidine-tagged proteins were purified using a Talon cobalt affinity resin, and the desired protein was eluted with 100 mM imidazole. Protein concentrations were determined initially by the Bio-Rad Protein Assay (Bio-Rad Laboratories) followed by active site titration.¹⁷

RNA Preparation. Ec tRNA^{Pro} was transcribed using T7 RNA polymerase from the BstN1-linearized plasmid as described previously¹⁸ and purified by denaturing 12% polyacrylamide gel electrophoresis.

ATP-PP_i Exchange Assays. The ATP-PP_i exchange assay was performed at 37 °C according to the published method.¹⁹ The concentrations of proline and alanine ranged from 0.025 to 50 mM and from 1 to 850 mM, respectively. The enzyme concentrations used were 10–20 nM for proline and 250–500 nM for alanine activation. Kinetic parameters were determined from Lineweaver–Burk plots and represent the average of at least three determinations.

ATP Hydrolysis Assays. ATP hydrolysis reactions for monitoring pretransfer editing were conducted as described previously.¹¹ An alanine concentration of 500 mM was used and a proline concentration of 30 mM. The reactions were initiated with a final ProRS concentration of 0.5 μ M.

Aminoacylation Assays. Aminoacylation assays were performed under standard conditions²⁰ with 0.5 μ M tRNA^{Pro}, 13.3 μ M [³H]proline, and 100 nM ProRS.

Aminoacylated tRNA. Aminoacylated tRNA for use in deacylation assays was prepared at room temperature according to published conditions.¹ Ec AlaRS (2 μ M) was used to acylate G1:C72/U70 tRNA^{Pro} (8 μ M) in the presence of [³H]Ala (7.3 μ M) in buffer containing 50 mM HEPES (pH 7.5), 4 mM ATP, 25 mM MgCl₂, 20 mM β -mercaptoethanol, 20 mM KCl, and 0.1 mg/mL bovine serum albumin.

Deacylation Assays. Deacylation assays were conducted at room temperature according to published conditions.¹ Reaction mixtures contained 1 μ M G1:C72/U70 [³H]Ala-tRNA^{Pro}, 150 mM KPO₄ (pH 7.0), 5 mM MgCl₂, and 0.1 mg/mL bovine serum albumin. The reactions were initiated with 5 μ M ProRS. Negative controls were performed using 150 mM KPO₄ (pH 7.0) in place of ProRS.

COMPUTATIONAL METHODS

Molecular Dynamics Simulations. MD simulations were conducted starting with the crystallographic structure of Ef ProRS [chain B, PDB entry 2J3M (open, residues 19–565)]. The Δ INS (constructed by replacing INS residues 232–394 with a 16-residue Gly₁₂Ser₄ linker¹¹) and the three mutants (G217A, E218A, and E218D) were generated with the Mutator plug-in of Visual Molecular Dynamics (VMD) version 1.8.6.²¹ For all simulations, the all-atom CHARMM22 force field²² was used within the NAMD²³ package. The three-point charge TIP3P model²⁴ was used to represent solvent water. Non-

bonded interactions were truncated using a switching function between 10 and 12 Å, and the dielectric constant was set to unity. The SHAKE algorithm²⁵ was used to constrain bond lengths and bond angles of water molecules and bonds involving a hydrogen atom. The MD simulations were performed using isothermal–isobaric (NPT) conditions. Periodic boundary conditions and particle mesh Ewald methods²⁶ were used to account for the long-range electrostatic interactions. In all MD simulations, a time step of 2 fs was used. The pressure of the system was controlled by the implementation of the Berendsen pressure bath coupling²⁷ as the temperature of the system was slowly increased from 100 to 300 K. During the simulations at 300 K, the pressure was kept constant by applying the Langevin piston method.^{28,29}

The WT and mutant proteins were solvated with water in a periodic rectangular box with dimensions of 130 Å \times 78 Å \times 92 Å with water padding of 12 Å between the walls of the box and the nearest protein atom. The charge neutralization (with sodium ions) of the solvated system was performed with the VMD autoionize extension.²¹ The resultant systems, containing ~84000 atoms (~74000 atoms for Δ INS ProRS), including approximately 16450 water molecules and 33 sodium ions (32 and 14 ions for E218A and Δ INS ProRS, respectively), were equilibrated by slightly modifying previously described procedures.^{30,31} Briefly, solvated proteins were further subjected to 1000 steps of conjugate gradient minimization at 100 K. The temperature of the solvated systems was then increased to 300 K in 3000 steps and was further equilibrated at 300 K for 500 ps. The equilibrated system was then used in 12 ns simulations. The equilibration and stability of the dynamics were checked by calculating the root-mean-square deviations (rmsds) of C α atoms from their initial coordinates.

Essential Dynamics. The collective dynamics of the protein was studied through essential dynamic analysis,^{32–34} which involves computation of the principal components of atomic fluctuations. The last 7 ns of the 12 ns MD simulation data was used to extract the principal modes of collective dynamics (called principal components) using Carma.³⁵ The mathematical operation behind essential dynamics is called principal component analysis (PCA), which takes a data set from a trajectory of a long time-scale MD simulation as input and extracts the low-frequency (high-amplitude) collective motions of the biomolecule, which are often more relevant for its functions.³⁶ The principal components were computed by performing eigenvalue decomposition of a covariance matrix, and the mathematical formalism is described elsewhere.³⁷ Briefly, the covariance matrix, **C** is computed with elements C_{ij} for any two points (C α coordinates) *i* and *j* using

$$C_{ij} = \langle (x_i - \langle x_i \rangle)(x_j - \langle x_j \rangle) \rangle \quad (1)$$

where $x_1, x_2, \dots,$ and x_{3N} are the mass-weighted Cartesian coordinates of an *N*-particle system and the angular brackets represent an ensemble average calculated over all sampled structures from the simulations. Next, the symmetric 3*N* \times 3*N* matrix **C** can be diagonalized with an orthonormal transformation matrix **R**

$$\mathbf{R}^T \mathbf{C} \mathbf{R} = \text{diag}(c_1, c_2, \dots, c_{3N}) \quad (2)$$

where $c_1, c_2, \dots,$ and c_{3N} are eigenvalues; columns in transformation matrix **R** are eigenvectors, which are also called the principal modes. If $X(t)$ represents the time-evolved 241

Table 1. Kinetic Parameters for Amino Acid Activation by WT, E218A, and G217A Ec ProRS^a

	amino acid	k_{cat} (s ⁻¹)	K_M (mM)	k_{cat}/K_M (s ⁻¹ mM ⁻¹)	relative k_{cat}/K_M	fold change
WT	proline	12.7 ± 4.9	0.228 ± 0.028	55.7	1	–
	alanine	3.52 ± 2.1	685 ± 360	0.00513	1	–
E218A	proline	4.4 ± 2.2	3.40 ± 0.68	1.29	0.0232	43
	alanine	3.26 ± 5.4	1360 ± 1300	0.0024	0.468	2
G217A	proline	3.37 ± 1.1	0.427 ± 0.077	7.89	0.142	7
	alanine	2.18 ± 0.23	454 ± 78	0.0048	0.935	0

^aResults are the average of three trials with the standard deviation indicated. In each, the k_{cat}/K_M of the mutant is relative to the WT kinetics with the corresponding amino acid.

242 coordinates (trajectory) of the water-encapsulated protein
243 active site, it can be projected onto the eigenvectors

$$q = \mathbf{R}^T[X(t) - \langle X \rangle] \tag{3}$$

244 The projection is a measure of the extent to which each
245 conformation is displaced, in the direction of a specific principal
246 mode, and is called the principal component (PC). For a
247 trajectory, the projections are obtained as matrix elements $q_i(t)$
248 ($i = 1, 2, \dots, M$).

249 PCA was conducted using the following steps: (i) preparing a
250 modified trajectory file by removing the coordinates of the
251 water molecules, selecting only the C_α atoms, and removing the
252 overall translational and rotational motions, (ii) calculating the
253 covariance matrix in which the atomic coordinates are the
254 variables, and (iii) diagonalizing the covariance matrix for
255 calculation of the eigenvectors and the corresponding
256 eigenvalues. The first three PCs were used for performing
257 PCA-based cluster analysis as discussed in Carma documenta-
258 tion.³⁵ Briefly, on the basis of contributions of the first three
259 PCs, conformations in the overall trajectory were grouped into
260 several clusters. The cluster with the greatest number of
261 conformations is representative of predominant conformational
262 fluctuations and was used for further analysis of dynamic cross-
263 correlations between C_α atoms. The cross-correlation coef-
264 ficient between fluctuations of residues i and j (CC_{ij}) was
265 calculated using

$$CC_{ij} = \frac{\langle (x_i - \langle x_i \rangle)(x_j - \langle x_j \rangle) \rangle}{\sigma_{x_i} \sigma_{x_j}} \tag{4}$$

266 where σ_{x_i} and σ_{x_j} represent the standard deviation of the
267 displacements of the two points (C_α coordinates) i and j ,
268 respectively. The correlated motion ($CC_{ij} > 0$) between two C_α
269 atoms occurs when they move in the same direction, while the
270 anticorrelated motion is generated when two C_α ($CC_{ij} < 0$)
271 atoms move in opposite directions.

272 The root-mean-square projections (rmsp) of q were obtained
273 from the last 7 ns of the simulations using the following
274 equation:

$$\text{rmsp} = \sqrt{\frac{1}{M} \sum_{i=1}^{\text{conf}} [q_i(t)]^2} \tag{5}$$

275 To determine if the functional dynamics had undergone
276 significant change because of a single-point mutation, a
277 combined essential dynamics analysis was performed following
278 literature methods.^{32–34} In this procedure, a comparison of
279 dynamics of five protein systems was conducted by
280 concatenating their trajectories to produce a combined
281 covariance matrix. The separate trajectories were then projected

onto the resulting eigenvectors, and the properties of these
projections were compared for these simulations.

RESULTS

The results are presented in the following order. First, the
experimental results are reported to show the impact of
mutation of the two strongly conserved noncatalytic residues
on the enzyme function. Next, the results of the MD
simulations are presented to illustrate the flexibility of the
ProRS and the overall coupling of various structural elements
surrounding its catalytic site. Finally, the molecular-level impact
of mutations (deletion and site-directed mutations) on the
catalytically important PBL dynamics was characterized
through essential dynamics analysis.

Activation of Proline and Alanine. To investigate the
role of the ²¹⁷GED²¹⁹ motif in maintaining coupled motions
among the protein segments surrounding the synthetic active
site, the effect of mutation of G217 and E218 on the function of
the enzyme was experimentally tested. The kinetic parameters
for proline and alanine activation were determined for both
mutants and compared with those of WT Ec ProRS. We found
that E218A ProRS activates proline but with a decreased k_{cat} (3-
fold) and an elevated K_M [15-fold (Table 1)]. Overall, the
proline activation efficiency of this mutant was decreased 45-
fold compared to that of the WT enzyme. Reduced catalytic
efficiency for proline activation was also observed for the
G217A mutant. The k_{cat}/K_M of G217A ProRS was reduced 7-
fold relative to that of the WT enzyme (Table 1). In contrast,
alanine activation by the G217A mutant was not affected
compared to that of the WT enzyme, and an only 2-fold
decrease in the extent of alanine activation was observed for the
E218A mutant (Table 1).

Aminoacylation of tRNA^{Pro}. The effect of mutation of
G217 and E218 on aminoacylation of proline was also tested.
Both G217A and E218A can charge proline onto tRNA^{Pro},
albeit with 3-fold reduced efficiency (Figure 3a).

Pretransfer Editing. Stimulation of ATP hydrolysis is
considered indicative of pretransfer editing, presumably because
the noncognate amino acids that are hydrolytically edited are
repeatedly reactivated by the synthetase, consuming ATP in
each cycle.³⁸ In contrast, the cognate amino acid is bound to
the synthetase until it is transferred to the tRNA. Ec ProRS
possesses tRNA-independent pretransfer editing against
alanine.³⁹ Here, we tested the pretransfer editing activity of
the two mutant proteins and compared them with the WT
activity. ATP hydrolysis was stimulated in the presence of
alanine for both mutants. However, E218A ProRS exhibited
reduced activity (9-fold) compared to that of the G217A
variant, which possessed editing activity that was comparable to
that of the WT enzyme (Figure 3b). The reduced activity of 330

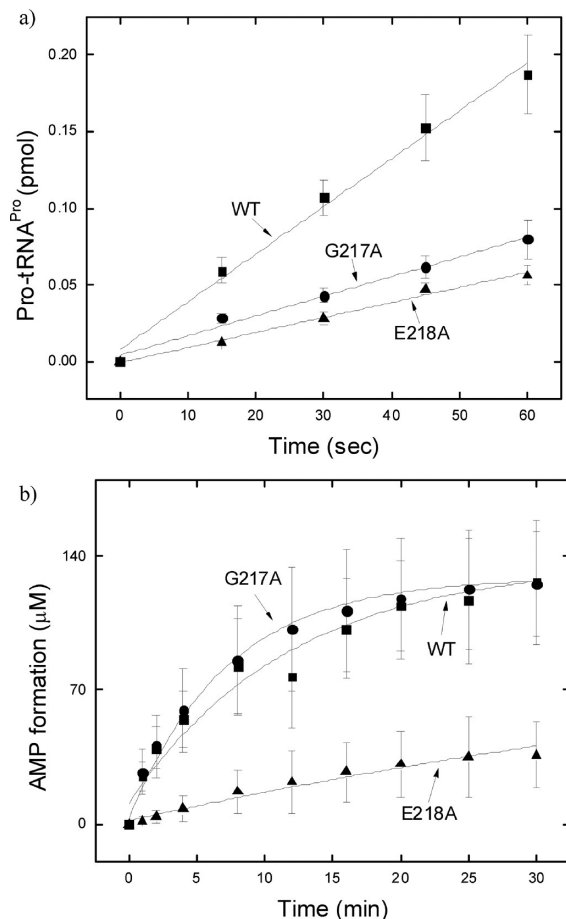


Figure 3. (a) Aminoacylation of tRNA^{Pro} with proline by WT, G217A, and E218A Ec ProRS. The assay was performed at 37 °C with 0.5 μM tRNA^{Pro} and 100 nM Ec ProRS. (b) Pretransfer editing in the presence of alanine by WT, G217A, and E218A Ec ProRS. The assay was performed at 37 °C using 0.5 μM ProRS and 500 mM alanine. Lines are single-exponential fits of the data.

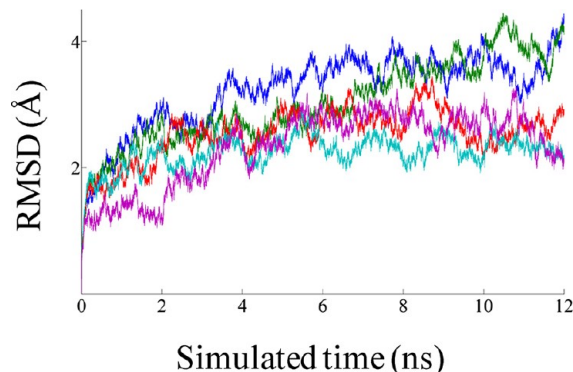


Figure 4. rmsds of the C_α atoms from their initial coordinate as a function of time. Calculations of rmsds for WT (blue), G217A (green), E218A (red), E218D (cyan), and ΔINS (purple) Ef ProRS were performed using 12 ns MD simulation data.

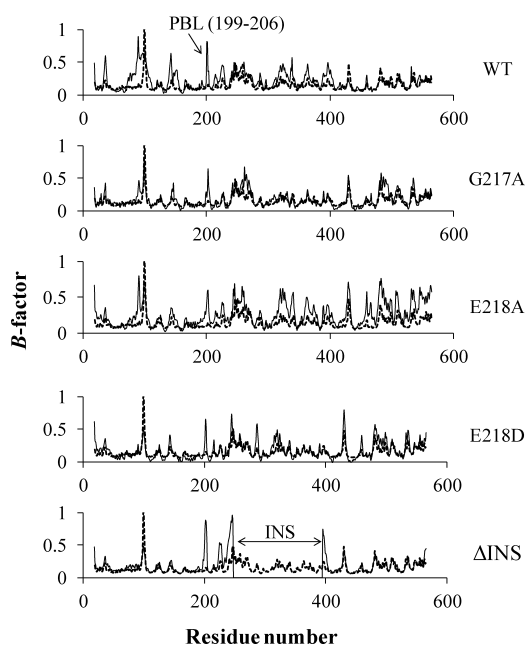


Figure 5. Comparison of the normalized C_α B factors obtained from the crystal structure (gray dotted line; PDB entry 2J3M, chain B) and calculated from MD simulation data (black solid line). For ΔINS, the calculated B factors are missing for residues 232–394.

331 E218A ProRS may, in part, be due to its poor alanine activation
332 efficiency.

333 **Post-Transfer Editing.** The post-transfer editing activity of
334 WT and variant ProRSs was also tested by monitoring the
335 hydrolysis of misacylated Ala-tRNA^{Pro}. All three enzymes
336 exhibited similar post-transfer editing activity (Figure S1 of
337 the Supporting Information). Thus, the binding of the
338 mischarged tRNA in the editing active site and the hydrolysis
339 of the ester bond were not affected by mutations at the editing
340 domain–activation domain interface.

341 **Root-Mean-Square Deviation (rmsd) Profiles.** The
342 rmsds were calculated using 12 ns MD simulation data for
343 WT, G217A, E218A, E218D, and ΔINS ProRS systems. The
344 plots of rmsd with respect to the initial equilibrated structure
345 are shown in Figure 4. After ~5 ns simulations, the C_α rmsd
346 values remained within ~1 Å. Data from the last 7 ns
347 simulations were used for further study.

348 **Flexible Regions.** B factor analysis revealed several highly
349 flexible regions in Ef ProRS. A plot of normalized experimental
350 B factors (crystallography¹⁴) and calculated B factors (using
351 Carma³⁵) of the C_α atoms of WT Ef ProRS is shown in Figure
352 5. The flexible regions identified by both experimental and
353 computational methods are comparable, except for residues
354 75–125 and the PBL. It appears that the flexibility of these two

regions is experimentally underestimated, possibly because of the
355 crystal packing arrangement of the protein. 356

In the case of the two mutants obtained by conservative
357 mutation, G217A and E218D, the overall protein flexibility was
358 reduced compared to that of the WT enzyme (Figure 5). 359
However, the substitution of E218 with alanine resulted in the
360 increased flexibility of the protein backbone, especially for the
361 C_α atoms of the INS and C-terminal domain. Interestingly, in
362 all three mutants (G217A, E218A, and E218D), the flexibility
363 of the PBL was reduced compared to that of the WT protein. 364
On the other hand, the complete deletion of the INS resulted
365 in a less flexible protein with B factors almost comparable to the
366 experimentally observed results except for the PBL, which
367 becomes more flexible in the absence of the INS (Figure 5). 368

369 **Dynamic Cross Correlations and Essential Dynamics**
370 **Analyses.** The dynamic cross-correlation map obtained from
371 the MD simulation of Ef ProRS (chain B) is shown in Figure 6. 371
In this study, the dynamic cross-correlation matrix was 372

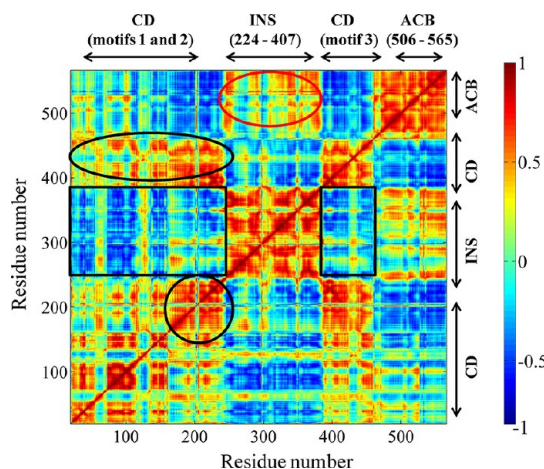


Figure 6. Dynamic cross-correlations between the C_{α} atoms of Ef ProRS obtained from the cluster analysis and PCA. A value of +1.0 was set for strongly correlated motion (red), whereas -1.0 was used for strongly anticorrelated motions (blue). The boxed and circled regions are discussed in the text. Abbreviations: CD, catalytic domain; INS, insertion domain; ACB, anticodon binding domain.

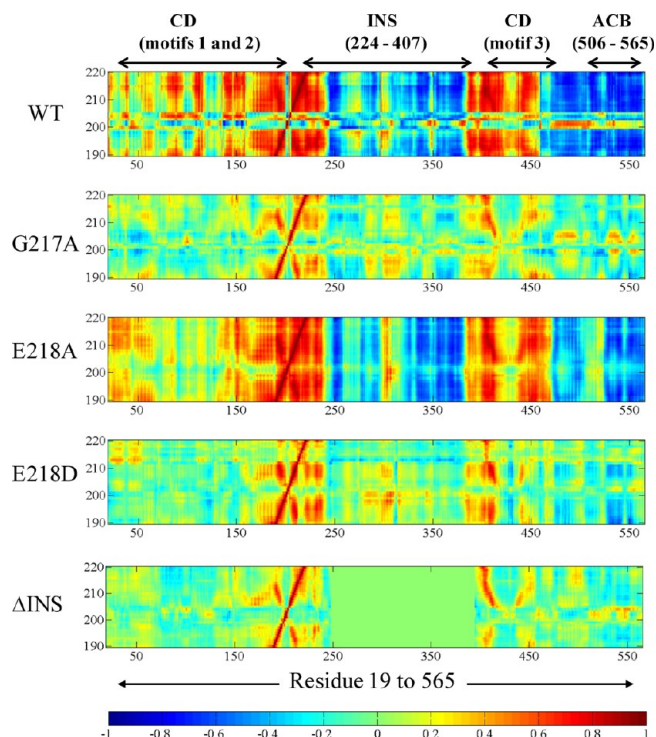


Figure 7. Dynamic cross-correlations between the C_{α} atoms of the PBL-containing protein segment (residues 190–220) vs C_{α} atoms of residues 19–565 of the WT and mutant ProRSs. Color coding is as described in the legend of Figure 6. For Δ INS, the region for the cross-correlations between residues 190–220 and INS residues 247–394 is shown in a green rectangle. Residues 232–394 are replaced with a 16-residue linker in this plot.

373 generated using the first three PCs. Analysis of the cross-
 374 correlation of fluctuations of residues for the first three PCs
 375 revealed both inter- and intradomain motional correlation. It
 376 was found that the activation domain and the INS are mainly
 377 engaged in anticorrelated motions; i.e., their displacements are
 378 in opposite directions [$CC_{ij} < 0$ (Figure 6, black rectangles)].
 379 An anticorrelated pattern of motions was also observed
 380 between the catalytic domain residues and the anticodon
 381 binding elements of Ef ProRS. On the other hand, the motion
 382 of the editing domain and the anticodon binding domain is
 383 weakly correlated [$CC_{ij} > 0$ (Figure 6, red oval)].

384 Various structural elements within the catalytic domain,
 385 which are essential for substrate binding and catalysis, are
 386 engaged in correlated motions (Figure 6, black oval). As
 387 expected, the adjacent residues of the protein segment
 388 (residues 190–220) containing the PBL and the $^{217}\text{GED}^{219}$
 389 motif are engaged in strong correlated motion (Figure 6, black
 390 circle). Also, the motion of the PBL-containing protein
 391 segment is mostly correlated in nature with respect to motifs
 392 1–3 of the catalytic domain. However, its motion is
 393 anticorrelated with respect to the INS and the anticodon
 394 binding domain.

395 The effect of deletion of INS and point mutation of G217
 396 and E218 on Ef ProRS dynamics was also studied. The dynamic
 397 cross-correlation map of the atomic (C_{α}) fluctuations between
 398 the PBL-containing protein segments (residues 190–220) and
 399 the rest of the molecule for the WT and the mutant variants is
 400 shown in Figure 7. Although we cannot rule out the change in
 401 structure due to these mutations (site-directed/deletion),
 402 noticeable alteration of residue fluctuations between the PBL-
 403 containing protein segment and other structural elements of the
 404 protein was observed for all mutant proteins compared to the
 405 WT enzyme (Figure 7). In particular, a significant change in the
 406 motional coupling between the PBL-containing segment and
 407 the editing domain (residues 224–407) was observed for the
 408 two ProRS variants, G217A and E218D. In addition, noticeable
 409 alteration of dynamic coupling among residues of the entire
 410 PBL-containing segment (residues 190–235) and residues
 411 150–235 as well as anticodon binding domain was observed
 412 (Figure 7).

Combined Essential Dynamics. To examine the impact 413
 of the deletion of INS or point mutation in the $^{217}\text{GED}^{219}$ motif 414
 on the collective dynamics of the PBL, we analyzed the 415
 essential dynamics of WT Ef ProRS and mutant variants using 416
 the last 7 ns of the 12 ns MD simulation data. Specifically, we 417
 performed a “combined” essential dynamics analysis,^{32,33} using 418
 the concatenated trajectories (of the C_{α} atoms) of all five 419
 proteins (WT, Δ INS, G217A, E218A, and E218D). 420

The combined essential dynamics analysis clearly shows that 421
 each mutation has an impact on the collective PBL (residues 422
 190–210) dynamics. The rmsf’s (eq 5) as a function of 423
 eigenvector indices for the WT and mutant proteins of Ef 424
 ProRS are shown in Figure 8. The fluctuation of the PBL along 425
 PC1 is significantly altered for all the mutant proteins 426
 compared to that of the WT enzyme. Noticeable changes 427
 were also observed for PC2 and PC3. Therefore, this analysis 428
 indicates that the deletion of the INS or mutation at the 429
 junction of the INS and activation domain could impact PBL 430
 dynamics and potentially alter substrate binding. Similar 431
 differences in the slow dynamics of the PBL upon mutation 432
 of G217 and E218 to alanine were observed for Ec ProRS 433
 (Figure S2 of the Supporting Information). 434

The alteration of the dynamics of the PBL either due to the 435
 deletion of the INS or due to mutations in the $^{217}\text{GED}^{219}$ motif 436
 can be visualized from the superimposition of conformations of 437
 the PBL extracted from the essential dynamics analysis. These 438
 superimposed conformations correspond to the dynamics of 439
 the PBL along the three PCs (i.e., in the direction of collective 440
 dynamics) and are displayed in Figure 9. Only backbone C_{α} 441
 atoms are shown for the sake of clarity. In the C_{α} traces, it is 442

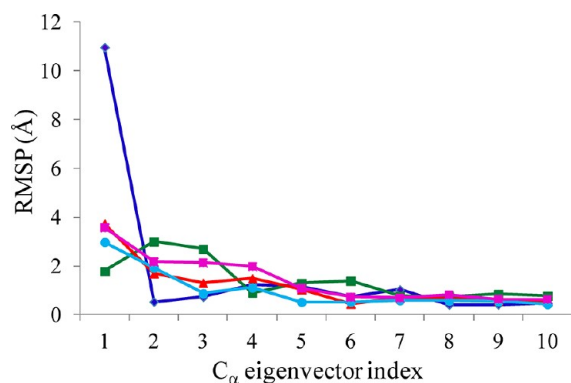


Figure 8. Combined analysis of the computed root-mean-square projections (rmsp, eq 5) over the last 7 ns of 12 ns simulation data for eigenvectors 1–10 for WT (blue), G217A (green), E218A (red), E218D (cyan), and ΔINS (purple) Ef ProRS.

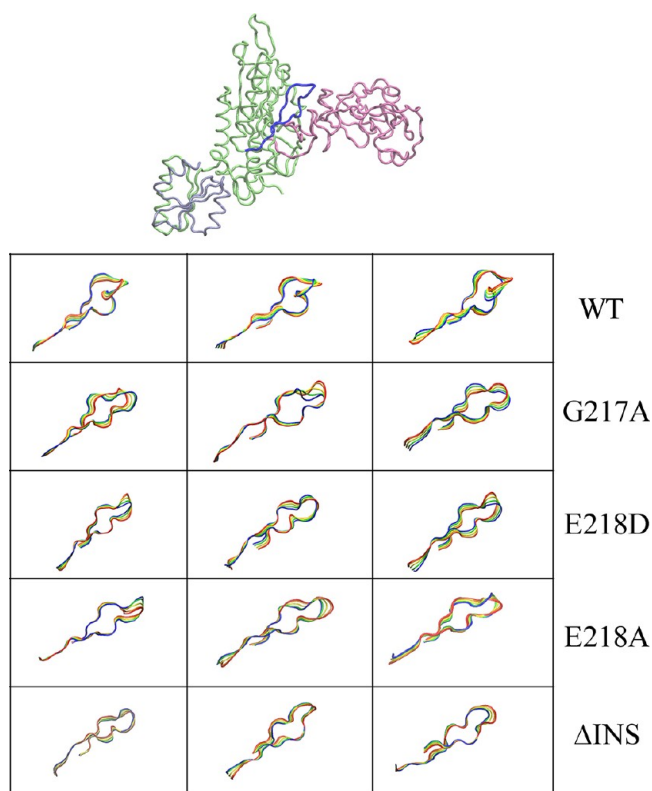


Figure 9. Visual representation of the movement of the PBL. Superposition of four configurations extracted from the concatenated trajectories by projecting the C_{α} motion onto eigenvectors 1–3. The four conformations are colored blue (starting), green, yellow, and red (end).

443 apparent that the pattern of the collective dynamics of the PBL
 444 (along the first three PCs) was altered by the point mutation at
 445 the domain–domain interface as well as by the deletion of the
 446 INS. Taken together, combined essential dynamics analysis
 447 revealed that deletion of INS or point mutations at the catalytic
 448 domain–editing domain junction caused perceptible changes in
 449 the collective PBL dynamics.

450 ■ **DISCUSSION**

451 **Protein Dynamics and Catalysis.** Dynamics is an intrinsic
 452 property, encrypted in the three-dimensional structure and

folding of a protein. Collective dynamics are prevalent in 453
 modular proteins and play an important role in enzyme 454
 function. In fact, simulations of mechanochemical properties of 455
 enzymes have shown that coupling between catalytic function 456
 and collective dynamics is a prerequisite for enzyme activity.⁴⁰ 457
 Several other studies have also revealed that internal motions 458
 essentially represent the intrinsic mechanical properties of an 459
 enzyme and do not originate from the presence of a substrate. 460
 Nevertheless, these internal protein motions facilitate substrate 461
 recognition and binding and thereby promote catalysis.^{41–43} 462
 In addition, studies have demonstrated that protein motions can 463
 modify the catalytic rate by influencing the height of the 464
 activation free energy barrier and the transmission coefficient 465
 (i.e., the capacity of recrossing the barrier).^{44–46} For example, a 466
 direct correlation between the frequencies of enzyme motions 467
 and catalytic turnover rates was observed in cyclophilin A using 468
 NMR relaxation experiments.⁴⁶ 469

A number of studies indicate that internal protein motions 470
 involve networks of residues extending beyond the catalytic 471
 site.^{41,44,45} Enzyme catalysis is found to be augmented by 472
 coupled motion through these networks amidst growing 473
 evidence that the slower collective protein motions and the 474
 faster bond-breaking or -forming motions are connected. An 475
 example of such a synergistic relationship can be found in 476
 adenylate kinase,⁴⁷ where faster (pico- to nanosecond time 477
 scale) atomic fluctuations at the hinge regions were found to 478
 promote the large-scale displacement of the lid during substrate 479
 binding. Also, studies of several enzymes, including dihydrofo- 480
 late reductase and liver alcohol dehydrogenase,^{42,45,48} have 481
 demonstrated that mutations of noncatalytic residues alter their 482
 catalytic function by modifying internal enzyme motions. 483
 Taken together, there is an overwhelming amount of evidence 484
 showing the significance of coupled dynamics in enzyme 485
 function. The role of coupled dynamics in the structure and 486
 function of ProRS has remained unexplored and constitutes the 487
 basis of this investigation. 488

Proposed Role of the Editing Domain. To probe the 489
 hypothesis that the collective dynamics involving the editing 490
 domain regulate substrate binding and catalysis by ProRS, the 491
 motion of ΔINS construct was compared with that of the full- 492
 length WT enzyme. In addition, two noncatalytic but conserved 493
 residues (G217 and E218) in the editing domain–activation 494
 domain junction were chosen for mutagenesis. If coupled 495
 internal dynamics truly exists between structural elements in 496
 the vicinity of the PBL, then point mutations in any of these 497
 elements should alter the dynamics, as well as the efficiency, of 498
 catalysis. 499

Amino Acid Activation and Aminoacylation. Exper- 500
 imental studies show that G217 and E218 are critical for 501
 enzyme catalysis. The X-ray crystal structure of bacterial ProRS 502
 shows strong interactions between E218 and a conserved 503
 arginine residue [R151 of Ef ProRS (see Figure 1b)] that helps 504
 to stabilize the phosphate group of the substrate ATP 505
 molecule.¹⁴ Indeed, a 45-fold decrease in the level of proline 506
 activation was measured in the case of E218A ProRS, showing 507
 that this residue is critical for cognate amino acid activation. 508
 However, only a small decrease (~2-fold) in alanine activation 509
 efficiency was observed for this mutant. A 7-fold decrease in 510
 proline activation efficiency upon mutation of G217 to alanine 511
 was observed, although this residue does not interact directly 512
 with any catalytic site residues. The lack of a significant effect 513
 on alanine activation for the E218A and G217A variants 514
 suggests that these residues might aid in maintaining the 515

516 internal dynamics of the active site protein segments and the
517 PBL, which facilitates the binding of the cognate amino acid but
518 plays a more minor role in noncognate alanine activation. This
519 is also apparent from the fact that the k_{cat} for proline activation
520 by E218A ProRS was only reduced 3-fold, whereas the K_M was
521 elevated 15-fold.

522 The mutation of G217 and E218 to alanine also impacted
523 cognate tRNA aminoacylation (Figure 3a), although the impact
524 was less severe (~ 2 – 3 -fold) than for amino acid activation.
525 This observation suggests that the binding of the 3'-acceptor
526 end in the aminoacylation active site was not altered
527 significantly by the alanine substitutions.

528 **Role of PBL in Amino Acid Selection.** If the open to
529 closed conformational transition of the PBL is important for
530 the protection of the cognate aminoacyl adenylate from
531 spontaneous hydrolysis by the surrounding water, the mutation
532 of G217 and E218 to alanine may be expected to enhance Pro-
533 AMP hydrolysis. However, ATP hydrolysis was only slightly
534 stimulated in the presence of proline for the G217A and E218A
535 mutants (Figure S1a of the Supporting Information),
536 suggesting that the main role of the PBL is to facilitate
537 amino acid selection and binding. Moreover, no noticeable
538 difference in post-transfer editing activity was observed for
539 these mutants relative to that of the WT enzyme (Figure S1b of
540 the Supporting Information), demonstrating that mutations in
541 the $^{217}\text{GED}^{219}$ motif do not affect binding and hydrolysis of
542 misacylated tRNA^{Pro}.

543 **Flexibility and Collective Protein Dynamics.** The *B*
544 factor calculations performed on the Ef ProRS demonstrated
545 that the PBL is quite flexible (Figure 5). However, the flexibility
546 of this loop was altered by the mutation of G217 and E218. As
547 expected, mutation of G217 to alanine brought some rigidity to
548 the PBL dynamics. On the other hand, mutation of E218 to
549 alanine caused an increase in the mobility of the whole protein
550 backbone but reduced the flexibility of the PBL. The increased
551 mobility of the protein backbone is expected as the substitution
552 of E218 with alanine disrupted the electrostatic interaction
553 between E218 and R151 of the activation domain (Figure 1b).
554 Interestingly, the mutation of E218 to aspartic acid resulted in
555 an overall reduction in protein flexibility. Close scrutiny of the
556 E218D structure revealed the existence of some additional H-
557 bond interactions between the surrounding residues and the
558 aspartic acid, which might have brought some extra rigidity to
559 the structure (data not shown). However, the deletion of the
560 INS has the reverse effect on the flexibility of the PBL.
561 Apparently, the PBL that is essential for substrate binding and
562 catalysis acquired significant flexibility upon deletion of the INS
563 (Figure 5). This observation suggests that the INS might have a
564 role in maintaining the optimal flexibility of the PBL.

565 The cross-correlation matrix obtained from the cluster
566 analysis (eq 4) revealed that the editing domain is mainly
567 engaged in anticorrelated motion with the central activation
568 domain (Figure 6). The existence of anticorrelated motion
569 between these two domains may be critical for providing
570 adequate space for the 3'-end of a tRNA to enter the synthetic
571 active site for aminoacylation. Anticorrelated motion between
572 the editing and activation domains has also been observed in
573 other synthetase systems, including isoleucyl- and leucyl-tRNA
574 synthetases.^{49,50} Close analysis of the dynamic cross-correlation
575 matrix also revealed the existence of correlated motion among
576 several polypeptide segments within the activation domain. In
577 addition, the adjacent residues of the polypeptide segment that
578 includes both the PBL and the $^{217}\text{GED}^{219}$ motif (residues 195–

225) are found to be engaged in correlated motion among
579 themselves and anticorrelated motion with most of the editing
580 domain elements. Moreover, the simulated collective dynamics
581 analysis of the WT versus mutant ProRSs revealed that
582 mutation of noncatalytic residues and deletion of INS indeed
583 alter the dynamics of the PBL with respect to the rest of the
584 protein. Analysis of the dynamic cross-correlations between the
585 PBL and other amino acid residues of Ef ProRS (Figure 7)
586 demonstrated that the extent of correlation or anticorrelation
587 between residue fluctuations depends upon neighboring as well
588 as distant residues. It also showed that the anticorrelated
589 motion between the editing domain and PBL undergoes a
590 perceptible change in the case of the G217A, E218A, and
591 E218D variants. 592

The effect of alanine substitutions at G217 and E218 on the
593 PBL dynamics was also evident from the combined essential
594 dynamics analysis, which showed significant changes in the
595 rmsp of the first three major modes (eigenvectors) of collective
596 dynamics of the PBL (Figure 8). Interestingly, the combined
597 PC analysis shows the deletion of INS or mutation of G217 and
598 E218 has a comparable effect on the collective PBL dynamics
599 (Figures 8 and 9). Although these simulations were conducted
600 in the absence of substrate, the analysis suggests that mutation
601 of residues so close to the PBL has an impact on the movement
602 of the PBL as significant as that observed for the deletion of the
603 whole INS. Taken together, these observations suggest that
604 coupled dynamics are relevant for PBL movement and,
605 therefore, could impact substrate binding and catalysis. 606

Examination of the polypeptide segment (residues 190–220)
607 at the interface of the activation and editing domains reveals the
608 presence of a number of negatively charged residues, namely,
609 E209, E218, D219, E234, and E407 (Figure 10). These
610 residues, which are conserved in both Ef and Ec ProRSs, are 611

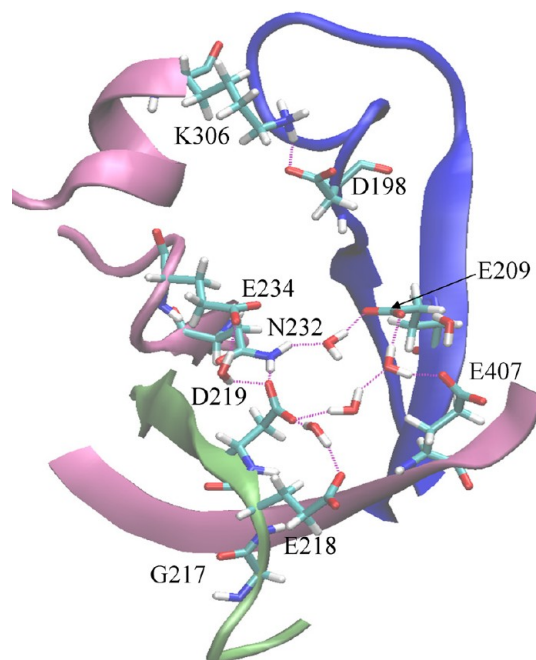


Figure 10. View of the region of Ef ProRS (PDB entry 2J3M, chain B) adjacent to the PBL and the “GED” motif showing charged residues at the activation domain–editing domain interface. The color coding is as follows: mauve for editing domain elements, blue for the PBL, and lime for the GED motif.

612 hydrogen-bonded to each other through water molecules and
 613 other polar residues like N232 and display significant
 614 correlations in the direction of their motions (Table 2).

Table 2. Correlation Coefficients (CC_{ij} , eq 4) of Fluctuations of Residue Pairs in Ef ProRS, Which Were Observed To Be Engaged in Hydrogen Bonding (Figure 10)

amino acid pair	CC_{ij}			
	WT	G217A	E218A	E218D
D219...E209	0.70	0.35	0.70	0.34
E218...E209	0.58	0.30	0.75	0.24
D219...N232	0.54	0.42	0.71	0.40
E209...N232	0.79	0.44	0.80	0.66
E209...E234	0.65	0.12	0.69	0.55
D219...E407	0.77	0.48	0.74	0.35
E218...E407	0.81	0.45	0.78	0.28
M202...T241	0.72	-0.01	0.09	0.03
G203...T241	0.73	0.13	0.01	-0.08
G203...D347	0.63	0.11	-0.09	0.10
M202...E352	0.62	-0.17	-0.10	-0.03
M202...S380	0.69	-0.10	-0.08	0.28
G203...E382	0.64	0.15	0.01	0.10
G203...D383	0.61	0.07	0.39	0.22
M202...E382	0.50	0.14	0.26	0.00
M202...D383	0.60	0.01	0.21	0.23

615 Interestingly, the dynamic correlations among these residues of
 616 the INS and the extended part of the PBL were maintained in
 617 the E218A variant, whereas correlations between these polar
 618 residues were significantly reduced in the case of G218A and
 619 E218D mutants (Table 2). On the other hand, analysis of the
 620 dynamic coupling between the tip of the PBL (M202 and
 621 G203) and several surrounding structural elements (residues
 622 239–244, 345–351, and 378–383) of the INS (not shown)
 623 revealed that the movements of these editing domain segments
 624 are significantly correlated to the tip of the PBL in the WT
 625 enzyme. However, these distant correlations are completely
 626 abolished in all three mutants (Table 2). These observations
 627 suggest that mutation of either G217 or E218 has a strong
 628 impact on the collective motion of the PBL despite their varied
 629 local impacts. Moreover, structural analysis of the WT and
 630 mutant enzymes revealed that INS protein segments are
 631 approximately 2–3 Å closer to the tip of the PBL (residues
 632 201–204) in the WT enzyme than in the mutant proteins.
 633 These neighboring structural elements appear to be critical for
 634 maintaining the coupled dynamics between the two functional
 635 domains, as well as the optimal flexibility of the PBL. Therefore,
 636 the observed dramatic effect on enzyme catalysis in the INS
 637 deletion mutant¹¹ is fully consistent with our results.

638 ■ CONCLUSIONS

639 The combined use of computer simulations and mutational
 640 analysis has allowed a better understanding of the role of
 641 domain dynamics in the enzymatic function of prokaryotic-like
 642 ProRSs (Figure 1). Experimental mutational studies of two
 643 conserved residues, G217 and E218 (Figure 2), revealed
 644 significantly reduced catalytic efficiency, while essential
 645 dynamics analysis of these mutant proteins showed a reduction
 646 in the collective dynamics of the catalytically important proline-
 647 binding loop. Overall, this study provides insights into the

interplay of coupled dynamics and enzyme catalysis in
 prokaryotic-like ProRSs.

The two point mutations, G217A and E218A, were found to
 significantly impact proline activation, indicating that these
 noncatalytic residues are crucial for function. The mutation of
 G217 and E218 to alanine only mildly impacted cognate tRNA
 aminoacylation. This observation suggests that the binding of
 the 3'-acceptor end in the aminoacylation active site was not
 altered significantly by these mutations.

MD simulations of three point mutants (G217A, E218A, and
 E218D) and the deletion mutant (Δ INS) demonstrated that
 the overall fluctuations of the backbone were impacted
 differently among these enzymes. A reduction in backbone
 fluctuation was evident in the case of G217A and E218D,
 indicating more rigidity in the structure, while for E218A, a
 more flexible backbone was observed. For Δ INS, an overall
 reduction in flexibility was noted amidst a sharp increase in the
 number of fluctuations in the PBL.

The collective motion of PBL was studied by performing
 dynamic cross-correlation analyses (Figure 6), which demon-
 strated that the editing domain in the wild-type enzyme and the
 three mutants (G217A, E218A, and E218D) is quite flexible
 and engaged in anticorrelated motion with the activation
 domain. Although the basic coupling pattern did not change,
 the extents of correlations and anticorrelations were found to
 vary, consistent with the trend observed in the B factor analysis.
 In the case of G217A and E218D, the overall correlation among
 the structural elements surrounding the PBL is decreased, while
 for E218A, it is increased (Figure 5). This study indicates the
 role of E218 is not only to stabilize the substrate, as proposed
 previously,¹⁴ but also to maintain PBL dynamics through
 coupled motion.

This study also provides insights into the severely reduced
 proline activation efficiency of Δ INS ProRS.⁵¹ In the case of
 this variant, the analysis of the collective dynamics of the PBL
 revealed a total abolition of the coupling of motions with
 surrounding elements. Removal of the editing domain disrupts
 the hydrogen bonding network between polar residues at the
 domain–domain interface, which is important for the
 maintenance of the coupled protein dynamics (Figure 10)
 and optimal flexibility of protein segments surrounding the
 activation site. Although only the ²¹⁷GED²¹⁹ motif was targeted
 here, the role of other noncatalytic residues, such as N232 and
 E234, in the editing domain of Ec ProRS can be explored in the
 future.

Taken together, this work provides an understanding of how
 noncatalytic residues in a distant site modulate the activity of
 prokaryotic-like ProRSs by maintaining the coupled protein
 dynamics essential for catalysis. This study also reveals a novel
 role for a synthetase editing domain and may explain why
 truncated or defunct editing domains have been maintained in
 some aminoacyl-tRNA synthetases, despite the lack of catalytic
 activity.^{51,52}

■ ASSOCIATED CONTENT

Supporting Information

Kinetic plots of pre- and post-transfer editing reaction and root-
 mean-square projections from essential dynamics analysis of
 WT and two mutants (G217A and E218A) of Ec ProRS. This
 material is available free of charge via the Internet at <http://pubs.acs.org>.

708 ■ AUTHOR INFORMATION

709 Corresponding Author

710 *S.B.: phone, (715) 836-2278; fax, (715) 836-4979; e-mail,
711 bhattas@uwec.edu. K.M.-F.: phone, (614) 292-2021; fax, (614)
712 688-5402; e-mail, musier@chemistry.ohio-state.edu. S.H.:
713 phone, (715) 836-3850; fax, (715) 836-4979; e-mail, hatis@
714 uwec.edu.

715 Funding

716 This work was supported in part by Teragrid [Grant TG-
717 DMR090140 (S.B.)], National Institutes of Health Grants
718 GM049928 (K.M.-F.) and GM085779 (S.H.), and the Office of
719 Research and Sponsored Programs of the University of
720 Wisconsin—Eau Claire.

721 Notes

722 The authors declare no competing financial interest.

723 ■ ACKNOWLEDGMENTS

724 We gratefully acknowledge the computational support from the
725 LTS, University of Wisconsin—Eau Claire. We thank Dr.
726 Stephen Cusack for providing the coordinates for the model of
727 Ec ProRS used in this work. We are also thankful to the three
728 anonymous reviewers for their constructive comments.

729 ■ ABBREVIATIONS

730 Ec, *E. coli*; ED, essential dynamics; Ef, *En. faecalis*; MD,
731 molecular dynamics; INS, insertion domain; PBL, proline-
732 binding loop; PCA, principal component analysis; PDB,
733 Protein Data Bank; ProRS, prolyl-tRNA synthetase; rmsd,
734 root-mean-square deviation; rmsp, root-mean-square projec-
735 tion; WT, wild-type.

736 ■ REFERENCES

737 (1) Beuning, P. J., and Musier-Forsyth, K. (2000) Hydrolytic editing
738 by a class II aminoacyl-tRNA synthetase. *Proc. Natl. Acad. Sci. U.S.A.*
739 97, 8916–8920.
740 (2) Beuning, P. J., and Musier-Forsyth, K. (2001) Species-specific
741 differences in amino acid editing by class II prolyl-tRNA synthetase. *J.*
742 *Biol. Chem.* 276, 30779–30785.
743 (3) Ahel, I., Stathopoulos, C., Ambrogelly, A., Sauerwald, A.,
744 Toogood, H., Hartsch, T., and Soll, D. (2002) Cysteine activation is
745 an inherent in vitro property of prolyl-tRNA synthetases. *J. Biol. Chem.*
746 277, 34743–34748.
747 (4) Mascarenhas, A., Martinis, S. A., An, S., Rosen, A. E., and Musier-
748 Forsyth, K. (2009) *Protein Engineering*, Vol. 22, Springer-Verlag, New
749 York.
750 (5) Stehlin, C., Burke, B., Yang, F., Liu, H., Shiba, K., and Musier-
751 Forsyth, K. (1998) Species-specific differences in the operational RNA
752 code for aminoacylation of tRNA^{Pro}. *Biochemistry* 37, 8605–8613.
753 (6) Cusack, S., Yaremchuk, A., Krikiliviy, I., and Tukalo, M. (1998)
754 tRNA^{Pro} anticodon recognition by *Thermus thermophilus* prolyl-
755 tRNA synthetase. *Structure* 6, 101–108.
756 (7) Wong, F. C., Beuning, P. J., Nagan, M., Shiba, K., and Musier-
757 Forsyth, K. (2002) Functional role of the prokaryotic proline-tRNA
758 synthetase insertion domain in amino acid editing. *Biochemistry* 41,
759 7108–7115.
760 (8) Wong, F. C., Beuning, P. J., Silvers, C., and Musier-Forsyth, K.
761 (2003) An isolated class II aminoacyl-tRNA synthetase insertion
762 domain is functional in amino acid editing. *J. Biol. Chem.* 278, 52857–
763 52864.
764 (9) An, S., and Musier-Forsyth, K. (2004) Trans-editing of Cys-
765 tRNA^{Pro} by *Haemophilus influenzae* YbaK protein. *J. Biol. Chem.* 279,
766 42359–42362.
767 (10) An, S., and Musier-Forsyth, K. (2005) Cys-tRNA^{Pro} editing
768 by *Haemophilus influenzae* YbaK via a novel synthetase-YbaK-tRNA
769 ternary complex. *J. Biol. Chem.* 280, 34465–34472.

(11) Hati, S., Ziervogel, B., Sternjohn, J., Wong, F. C., Nagan, M. C., 770
771 Rosen, A. E., Siliciano, P. G., Chihade, J. W., and Musier-Forsyth, K.
(2006) Pre-transfer editing by class II prolyl-tRNA synthetase: Role of
772 aminoacylation active site in “selective release” of noncognate amino
773 acids. *J. Biol. Chem.* 281, 27862–27872. 774
(12) Weimer, K. M., Shane, B. L., Brunetto, M., Bhattacharyya, S.,
775 and Hati, S. (2009) Evolutionary basis for the coupled-domain
776 motions in *Thermus thermophilus* leucyl-tRNA synthetase. *J. Biol.*
777 *Chem.* 284, 10088–10099. 778
(13) Bu, Z., Biehl, R., Monkenbusch, M., Richter, D., and Callaway,
779 D. J. (2005) Coupled protein domain motion in Taq polymerase
780 revealed by neutron spin-echo spectroscopy. *Proc. Natl. Acad. Sci.*
781 *U.S.A.* 102, 17646–17651. 782
(14) Crepin, T., Yaremchuk, A., Tukalo, M., and Cusack, S. (2006)
783 Structures of two bacterial prolyl-tRNA synthetases with and without a
784 cis-editing domain. *Structure* 14, 1511–1525. 785
(15) Burke, B., Lipman, R. S., Shiba, K., Musier-Forsyth, K., and Hou,
786 Y. M. (2001) Divergent adaptation of tRNA recognition by
787 *Methanococcus jannaschii* prolyl-tRNA synthetase. *J. Biol. Chem.* 276,
788 20286–20291. 789
(16) Stehlin, C., Heacock, D. H. II, Liu, H., and Musier-Forsyth, K.
790 (1997) Chemical modification and site-directed mutagenesis of the
791 single cysteine in motif 3 of class II *Escherichia coli* prolyl-tRNA
792 synthetase. *Biochemistry* 36, 2932–2938. 793
(17) Fersht, A. R., Ashford, J. S., Bruton, C. J., Jakes, R., Koch, G. L.,
794 and Hartley, B. S. (1975) Active site titration and aminoacyl adenylate
795 binding stoichiometry of aminoacyl-tRNA synthetases. *Biochemistry* 14,
796 1–4. 797
(18) Liu, H., and Musier-Forsyth, K. (1994) *Escherichia coli* proline
798 tRNA synthetase is sensitive to changes in the core region of
799 tRNA^{Pro}. *Biochemistry* 33, 12708–12714. 800
(19) Heacock, D., Forsyth, C. J., Shiba, K., and Musier-Forsyth, K.
801 (1996) *Bioorg. Chem.* 24, 273–289. 802
(20) Musier-Forsyth, K., Scaringe, S., Usman, N., and Schimmel, P.
803 (1991) Enzymatic aminoacylation of single-stranded RNA with an
804 RNA cofactor. *Proc. Natl. Acad. Sci. U.S.A.* 88, 209–213. 805
(21) Humphrey, W., Dalke, A., and Schulten, K. (1996) VMD: Visual
806 molecular dynamics. *J. Mol. Graphics* 14, 27–38. 807
(22) MacKerell, A. D. J., Bashford, D., Bellott, M., Dunbrack, R. L. J.,
808 Evanseck, J. D., Field, M. J., Fischer, S., Gao, J., Gou, J., Ha, S., Joseph-
809 McCarthy, D., Kuchnir, L., Kuczera, K., Lau, F. T. K., Mattos, C.,
810 Michnick, S., Ngo, T., Nguyen, D. T., Prodhom, B., Reiher, W. E. I.,
811 Roux, B., Schelenkrich, M., Smith, J. C., Stote, R., Straub, J., Watanabe,
812 M., Wiórkiewicz-Kuczera, J., Yin, D., and Karplus, M. (1998) All-atom
813 empirical potential for molecular modeling and dynamics studies of
814 proteins. *J. Phys. Chem. B* 102, 3586. 815
(23) Phillips, J. C., Braun, R., Wang, W., Gumbart, J., Tajkhorshid, E.,
816 Villa, E., Chipot, C., Skeel, R. D., Kale, L., and Schulten, K. (2005)
817 Scalable molecular dynamics with NAMD. *J. Comput. Chem.* 26, 1781–
818 1802. 819
(24) Jorgensen, W. L., Chandrasekhar, J., Madura, J. D., Impey, R.
820 W., and Klein, M. L. (1983) Comparison of simple potential functions
821 for simulating liquid water. *J. Chem. Phys.* 79, 926. 822
(25) Ryckaert, J. P., Ciotti, G., and Berendsen, H. J. C. (1977)
823 Numerical integration of the Cartesian equations of motion of a
824 system with constraints: Molecular dynamics of n-alkanes. *J. Comput.*
825 *Phys.* 23, 327–341. 826
(26) Darden, T., York, D., and Pedersen, L. (1993) Particle Mesh
827 Ewald: An N·Log(N) Method for Ewald Sums in Large Systems. *J.*
828 *Chem. Phys.* 98, 10089–10092. 829
(27) Berendsen, H. J. C., Postma, J. P., van Gunsteren, M. W. F.,
830 DiNola, A., and Haak, J. R. (1984) Molecular dynamics with coupling
831 to an external bath. *J. Chem. Phys.* 81, 3684–3690. 832
(28) Feller, S. E., Zhang, Y., Pastor, R. W., and Brooks, B. R. (1995)
833 Constant pressure molecular dynamics simulation: The Langevin
834 piston method. *J. Chem. Phys.* 103, 4613–4621. 835
(29) Martyna, G. J., Tobias, D. J., and Klein, M. L. (1994) Constant
836 pressure molecular dynamics algorithms. *J. Chem. Phys.* 101, 4177–
837 4189. 838

- 839 (30) Bhattacharyya, S., Ma, S., Stankovich, M. T., Truhlar, D. G., and
840 Gao, J. (2005) Potential of mean force calculation for the proton and
841 hydride transfer reactions catalyzed by medium-chain acyl-CoA
842 dehydrogenase: Effect of mutations on enzyme catalysis. *Biochemistry*
843 *44*, 16549–16562.
- 844 (31) Rauschnot, J. C., Yang, C., Yang, V., and Bhattacharyya, S.
845 (2009) Theoretical determination of the redox potentials of
846 NRH:quinone oxidoreductase 2 using quantum mechanical/molecular
847 mechanical simulations. *J. Phys. Chem. B* *113*, 8149–8157.
- 848 (32) Peters, G. H., van Aalten, D. M., Svendsen, A., and Bywater, R.
849 (1997) Essential dynamics of lipase binding sites: The effect of
850 inhibitors of different chain length. *Protein Eng.* *10*, 149–158.
- 851 (33) van Aalten, D. M., Amadei, A., Linssen, A. B., Eijssink, V. G.,
852 Vriend, G., and Berendsen, H. J. (1995) The essential dynamics of
853 thermolysin: Confirmation of the hinge-bending motion and
854 comparison of simulations in vacuum and water. *Proteins* *22*, 45–54.
- 855 (34) Mueller, R. M., North, M. A., Yang, C., Hati, S., and
856 Bhattacharyya, S. (2011) Interplay of flavin's redox states and protein
857 dynamics: An insight from QM/MM simulations of dihydronicotina-
858 mide riboside quinone oxidoreductase 2. *J. Phys. Chem. B* *115*, 3632–
859 3641.
- 860 (35) Glykos, N. M. (2006) Software news and updates. Carma: A
861 molecular dynamics analysis program. *J. Comput. Chem.* *27*, 1765–
862 1768.
- 863 (36) Amadei, A., Linssen, A. B., and Berendsen, H. J. (1993)
864 Essential dynamics of proteins. *Proteins* *17*, 412–425.
- 865 (37) Kazmierkiewicz, R., Czaplowski, C. C., Lammek, B., and
866 Ciarkowski, J. (1999) Essential Dynamics/Factor Analysis for the
867 Interpretation of Molecular Dynamics Trajectories. *J. Comput.-Aided*
868 *Mol. Des.* *13*, 21–33.
- 869 (38) Jabukowski, H., and Goldman, E. (1992) Editing of errors in
870 selection of amino acids for protein synthesis. *Microbiol. Rev.* *56*, 412–
871 429.
- 872 (39) Beuning, P. J., and Musier-Forsyth, K. (2001) Species-specific
873 differences in amino acid editing by class II prolyl-tRNA synthetase. *J.*
874 *Biol. Chem.* *276*, 30779–30785.
- 875 (40) Yang, L. W., and Bahar, I. (2005) Coupling between catalytic
876 site and collective dynamics: A requirement for mechanochemical
877 activity of enzymes. *Structure* *13*, 893–904.
- 878 (41) Tousignant, A., and Pelletier, J. N. (2004) Protein motions
879 promote catalysis. *Chem. Biol.* *11*, 1037–1042.
- 880 (42) Hammes-Schiffer, S., and Benkovic, S. J. (2006) Relating protein
881 motion to catalysis. *Annu. Rev. Biochem.* *75*, 519–541.
- 882 (43) Bakan, A., and Bahar, I. (2009) The intrinsic dynamics of
883 enzymes plays a dominant role in determining the structural changes
884 induced upon inhibitor binding. *Proc. Natl. Acad. Sci. U.S.A.* *106*,
885 14349–14354.
- 886 (44) Agarwal, P. K. (2005) Role of protein dynamics in reaction rate
887 enhancement by enzymes. *J. Am. Chem. Soc.* *127*, 15248–15256.
- 888 (45) Agarwal, P. K., Billeter, S. R., Rajagopalan, P. T., Benkovic, S. J.,
889 and Hammes-Schiffer, S. (2002) Network of coupled promoting
890 motions in enzyme catalysis. *Proc. Natl. Acad. Sci. U.S.A.* *99*, 2794–
891 2799.
- 892 (46) Eisenmesser, E. Z., Millet, O., Labeikovsky, W., Korzhnev, D.
893 M., Wolf-Watz, M., Bosco, D. A., Skalicky, J. J., Kay, L. E., and Kern, D.
894 (2005) Intrinsic dynamics of an enzyme underlies catalysis. *Nature*
895 *438*, 117–121.
- 896 (47) Henzler-Wildman, K. A., Lei, M., Thai, V., Kerns, S. J., Karplus,
897 M., and Kern, D. (2007) A hierarchy of timescales in protein dynamics
898 is linked to enzyme catalysis. *Nature* *450*, 913–916.
- 899 (48) Rajagopalan, P. T., Lutz, S., and Benkovic, S. J. (2002) Coupling
900 interactions of distal residues enhance dihydrofolate reductase
901 catalysis: Mutational effects on hydride transfer rates. *Biochemistry*
902 *41*, 12618–12628.
- 903 (49) Tukalo, M., Yaremchuk, A., Fukunaga, R., Yokoyama, S., and
904 Cusack, S. (2005) The crystal structure of leucyl-tRNA synthetase
905 complexed with tRNA^{Leu} in the post-transfer-editing conformation.
906 *Nat. Struct. Mol. Biol.* *12*, 923–930.
- (50) Silvan, L. F., Wang, J., and Steitz, T. A. (1999) Insights into
907 editing from an ile-tRNA synthetase structure with tRNA^{ile} and
908 mupirocin. *Science* *285*, 1074–1077. 909
- (51) SternJohn, J., Hati, S., Siliciano, P. G., and Musier-Forsyth, K. 910
(2007) Restoring species-specific posttransfer editing activity to a
911 synthetase with a defunct editing domain. *Proc. Natl. Acad. Sci. U.S.A.* 912
104, 2127–2132. 913
- (52) Lue, S. W., and Kelley, S. O. (2005) An aminoacyl-tRNA 914
synthetase with a defunct editing site. *Biochemistry* *44*, 3010–3016. 915